

230714

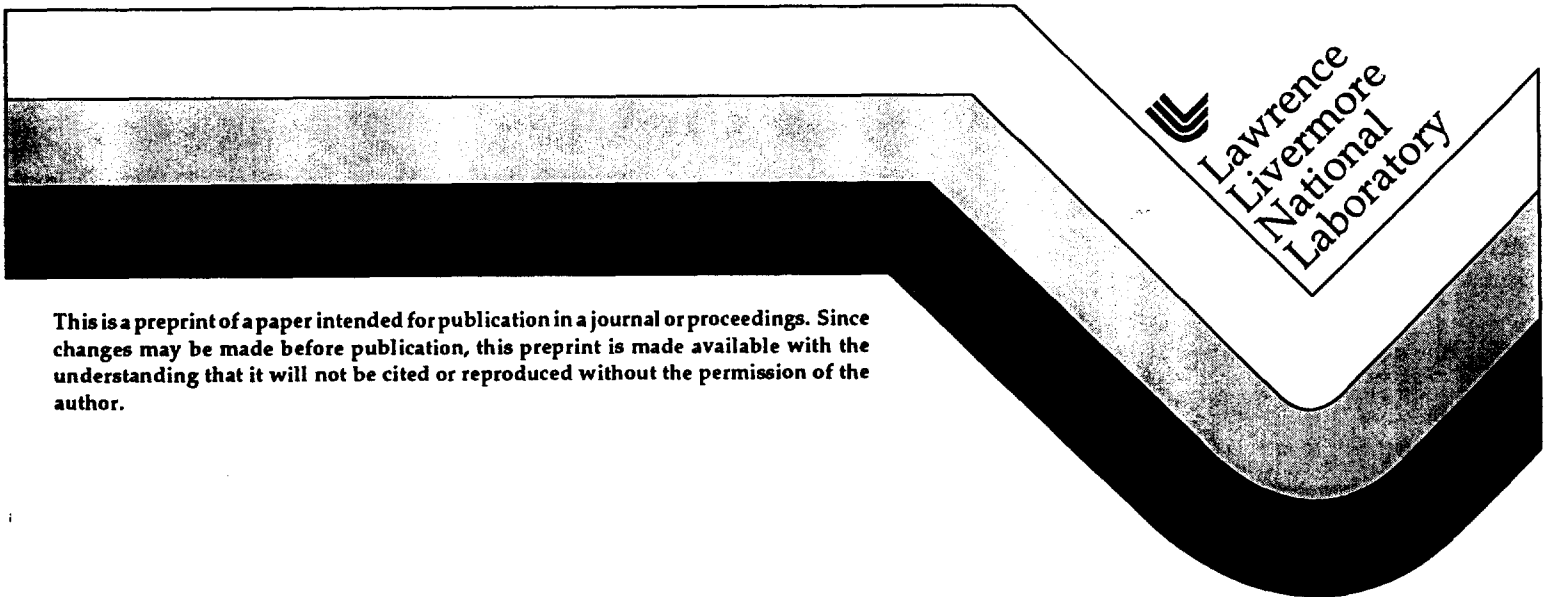
UCRL-JC-125223
PREPRINT

Techniques for Evaluation of E-Beam Evaporative Processes

Thomas C. Meier
Chris M. Nelson

This paper was prepared for submittal to the
Electron Beam Melting and Refining, State of the Art 1996
Reno, Nevada
October 23-25, 1996

October 1996



This is a preprint of a paper intended for publication in a journal or proceedings. Since changes may be made before publication, this preprint is made available with the understanding that it will not be cited or reproduced without the permission of the author.

DISCLAIMER

This document was prepared as an account of work sponsored by an agency of the United States Government. Neither the United States Government nor the University of California nor any of their employees, makes any warranty, express or implied, or assumes any legal liability or responsibility for the accuracy, completeness, or usefulness of any information, apparatus, product, or process disclosed, or represents that its use would not infringe privately owned rights. Reference herein to any specific commercial product, process, or service by trade name, trademark, manufacturer, or otherwise, does not necessarily constitute or imply its endorsement, recommendation, or favoring by the United States Government or the University of California. The views and opinions of authors expressed herein do not necessarily state or reflect those of the United States Government or the University of California, and shall not be used for advertising or product endorsement purposes.

TECHNIQUES FOR EVALUATION OF E-BEAM EVAPORATIVE PROCESSES

**Thomas C. Meier
Chris M. Nelson
Lawrence Livermore National Laboratory
P.O.Box 808, L-470
Livermore, CA 94550**

ABSTRACT

Efforts to evaluate and characterize electron beam evaporative processes at LLNL have produced a number of techniques and capabilities which have proven useful in advancing our process understanding. One of these diagnostic tools, high dynamic range video imaging of the molten pool surface, has provided insight regarding process responses at the melt pool liquid-vapor interface.

A water cooled video camera provides continuous high resolution imaging of the pool surface from a low angle position within 20 cm of the liquid-vapor interface. From this vantage point, the e-beam footprint is clearly defined and melt pool free surface shape can be observed. Effects of changes in e-beam footprint, power distribution and sweep frequency on pool surface shape and stability of vaporization are immediately shown.

Other electron beam melting and vaporization events have been observed and recorded. These include: formation of the pool and dissipation of "rafts" on the pool surface during startup, behavior of feed material as it enters the pool, effects of feed configuration changes on the mixing of feed entering the pool volume and behaviors of co-evaporated materials of different vapor pressures at the feed/pool boundary. When used in conjunction with laser vapor monitoring capabilities (presented at the 1994 Electron Beam Melting and Refining Conference, Reno, NV), correlation between pool surface phenomena and vaporizer performance has been identified.

This video capability was used in verifying the titanium evaporation model results presented at this conference by confirming the calculated melt pool surface deformations caused by vapor pressure of the departing evaporant at the liquid-vapor interface.

INTRODUCTION

High dynamic range video imaging, as applied by the Vapor Technology Group at Lawrence Livermore National Laboratory, has proven itself as a valuable tool for evaluation and development of electron beam melting and evaporation processes. Our increasing usage of this time-base correlated diagnostic capability as a component of a test instrumentation package has evolved with our capability to protect the camera when used in close proximity to the electron beam environment. The resulting high resolution video images have provided us useful insight for characterization of a wide range of process behaviors. These behaviors include: dynamics of feed entering the molten pool region, vapor source stability with changing e-beam power distribution, pool behavior under startup conditions, pool flow patterns and free surface shapes under steady-state operating conditions and observation of concurrent process phenomena, such as a cathodic arc discharge during e-beam operation.

The video segments which have been compiled from test records for this presentation are intended to illustrate the value of this video diagnostic capability.

HARDWARE CONFIGURATION

This video system uses an electronically shuttered CCD camera, housed in a water cooled enclosure, located within the vacuum vessel. Electronic shuttering provides an effective means to dynamically adjust the amount light energy converted to electrical charge at the CCD cells. This camera control, combined with appropriate filtering for the spectral content and intensity of light produced by test conditions, provides an high dynamic range of image attenuation for test conditions. Water cooling protects the camera electronics from thermal loads. Placing the camera within the vacuum vessel allows for high resolution imaging of conditions within the vaporizer, but subjects the camera to thermal load, vapor fluxes and transient electrical conditions. Careful accommodation of these conditions within the vacuum vessel has allowed us to maintain reliable performance from this camera system.

Figure 1 schematically shows a typical configuration used within the Evaporation Test Facility (ETF) at LLNL. It shows electron beam trajectory, melt location, and two primary camera locations within the ETF vessel. The low angle melt view camera is approximately 20 cm from melt centerline and points downward, approximately 10 degrees from horizontal, toward the melt surface. The remote camera is approximately 1 meter from the melt surface at approximately 45 degrees from horizontal.

Having identified these primary hardware components within the ETF vessel, the following sections describe the video segments that accompanied this presentation.

FLASH EVAPORATION OF ALUMINUM FROM NIOBIUM

This run was part of a test series to observe effects and verify limits for introducing a higher vapor pressure (and lower density) feed material into liquid metal pools. The test configuration is illustrated in Figure 2, where aluminum wire was fed into a molten niobium pool at a rate of 0.18 kg/hour (24 inches/minute). E-gun power was 112 kW and the corresponding niobium vaporization rate was 0.9 kg/hour. The vapor pressure of aluminum is 1,000,000 times greater than niobium at the melting temperature of niobium (2500 °C).

As shown in the video segment, aluminum wire that is fed over the far edge of the niobium melt is pushed back and resolidified on the far crucible wall. Some of this aluminum is remelted onto and vaporized from the solid niobium melt along the far edge of the crucible. Over the course of a few seconds, this aluminum forms a "beach" along the entire melt edge. The burst of aluminum vaporization that occasionally occurs when the aluminum feed wire contacts the liquid niobium surface propels that droplet violently away from the melt surface. The aluminum film boiling is analogous to the film boiling of water droplets on a hot skillet. The uncontrolled evaporation from the aluminum "beach" region on the niobium melt predominates the overall aluminum vapor distribution.

FLASH EVAPORATION OF ALUMINUM FROM TITANIUM

This run was a continuation the same test series, this time evaluating aluminum wire fed into a titanium melt at 0.56 kg/h (75 inches/minute). As shown in Figure 3, the e-gun power was approximately 50 kW and the corresponding titanium vaporization rate was 1.0 kg/h. The vapor pressure of aluminum is 200 times greater than titanium at the melting temperature of titanium (1800 °C).

As shown in the video segment, aluminum wire that is fed over the far edge of the titanium melt extends well over the liquid titanium pool before melting back to form a pendant droplet at the end of the aluminum wire feed. The aluminum pendant droplets grow to about 5 mm. diameter before falling to the melt surface about once every four to five seconds. The fallen droplets are

quickly swept back to the far pool edge by surface tension and buoyancy effects. A few of the droplets are ejected from the pool by the vapor pressure of the aluminum at the molten titanium temperature. There is also a visible accumulation of aluminum, oxide and other feed impurities at the far edge of the pool. It appears that limited aluminum-titanium mixing occurs within the field of view, and the resulting vapor deposition shows a skewing of the aluminum vapor distribution toward the wire feed end of the crucible. This suggests that aluminum-titanium mixing is restrained by the surface shear and buoyancy effects and that mixing across the pool is further inhibited by the short residence time of the higher vapor pressure aluminum material.

EVAPORATION OF ZIRCONIA

In this run, illustrated in Figure 4, a bottom fed 2.5 inch diameter bar of yttria stabilized zirconia was melted and vaporized in order to optimize this process for stable vaporization. A defocused circular swept e-beam, operated at 35 kW, was required to maintain stable vaporization. An average ZrO vaporization rate of 0.86 kg/hour was measured by diagnostic laser using molecular absorption technique.

As shown in the video, the liquid zirconia exhibits a very low viscosity, low density and an exceptionally high surface tension, making the pool very sensitive to e-beam position and power density variation on the melt pool surface.

TITANIUM MELT STARTUP

During this titanium melt model verification run series, two melt video segments were recorded concurrently from the two camera positions shown in Figure 5. The segments show the startup of a bottom fed, 3 inch diameter, titanium bar melt. A circular swept tightly focused e-beam was used. E-gun power was increased to 33.3 kW, achieving a titanium vaporization rate of 1.02 kg/hour.

The first video segment, from the remote camera location, shows a typical e-beam melt startup. The e-beam is initially formatted with a tight 1 inch diameter circular swept e-beam to form an apparently stable liquid pool. The sweep diameter is increased to 2 inches once the pool has formed, as directed by the run plan for this test.

The second video segment shows the same time sequence of events from the low angle camera view. This video segment presents a significantly different view of events. On forming the pool with the tight diameter circular swept e-beam, the vapor pressure of the evaporating titanium distorts the pool surface under the e-beam nearly to the point of pool instability. This near instability is further illustrated by the high velocities seen at the pool surface, particularly at the center where the converging pool flows cause the pool surface to bulge upward accommodate the volume of pool material. As the e-beam sweep diameter is increased to the steady-state operating format prescribed by the run plan, pool conditions become somewhat relaxed, but the pool still appears significantly more active than the remote camera view implies.

TITANIUM PLASMA ARC

During this test, a cathodic arc is struck between an anode and the surface of an e-beam heated titanium melt pool contained in a water cooled copper hearth. This test configuration, shown in Figure 6, has been the most severe test of the video camera electronics to date. During the test, e-gun power was approximately 50 kW with a corresponding titanium vaporization rate of 1.7 kg/hour. Concurrent cathodic arc current discharge was 500 amperes.

On establishing the continuous arc from melt to anode during e-beam vaporization, the e-beam focus and format reflect the cathodic arc effects on vapor ionization and magnetic field along the e-beam trajectory. The change in pool surface appearance from quiescent to somewhat turbulent is abrupt and obvious. A rotational stirring component is imparted to the titanium pool during continuous cathodic arc discharge.

ALUMINUM MELT STARTUP

This final pair of video segments show pool initiation and steady-state vaporization of an aluminum melt contained in a water cooled copper hearth. Test configuration is illustrated in Figure 7.

At the low e-beam power applied during startup (< 5kW), a very tranquil liquid film extends across the top surface of the aluminum melt directly under the e-beam footprint. Oxide and the low vapor pressure impurities are illuminated by the electron beam heating and are seen to float on the pool surface and spin as effected by surface tension and heating effects.

During steady-state aluminum vaporization, vapor rate is monitored by diagnostic laser using group velocity delay technique to assess laser light attenuation and determine aluminum vaporization rate. E-gun power is modulated between 63 and 80 kW for this test. The low angle, high resolution camera view shows stable aluminum vaporization at both power levels.

SUMMARY

In summary, this high dynamic range, high resolution video imaging capability developed for in-vessel viewing of the melt pool surface has provided us valuable insight into electron beam melting and vaporization processes. By improving camera reliability and integrating the camera into our process instrumentation, the camera has become an increasingly useful diagnostic tool and has proven its value in the analysis and characterization of a broad range of electron beam related processes.

ACKNOWLEDGMENT

I would like to take this opportunity thank my associates at LLNL, Thomas M. Anklam, Leon V. Berzins, David G. Braun, Glenn M. Heestand, Matthew A. McClelland and Jiri Jancarik for their technical support, Jonathan Storer and his associates at 3M for their collaborative contributions, and DARPA for support of this project. The work herein was performed under the auspices of the U.S. Department of Energy by Lawrence Livermore National Laboratory under contract No. W-7405-Eng-48.

This video system utilizes an electronically shuttered CCD camera housed in a water cooled enclosure



- Flexible camera positioning
- High resolution imaging
- Reliable performance

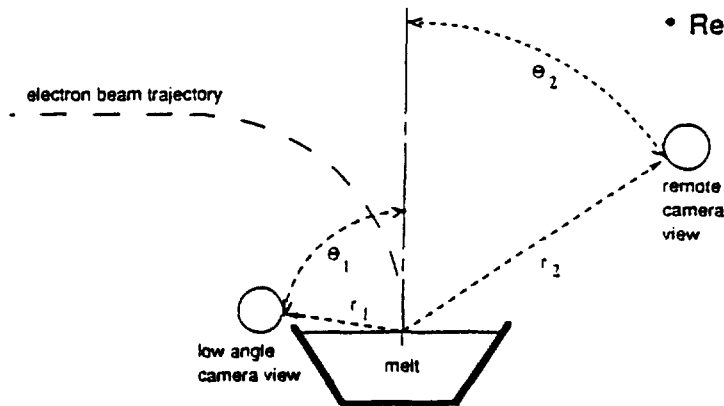
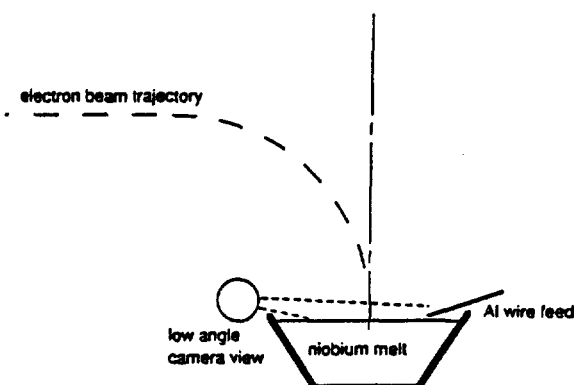


Figure 1

Flash evaporation of Aluminum from Niobium



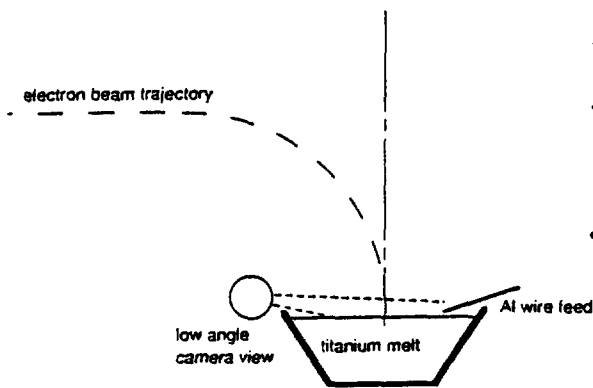
- E-gun power \cong 112 kW
- Nb vapor rate \cong 0.9 kg/h
(based on diagnostic laser;
verified by mass balance)
- Al wire feed rate \cong 0.18 kg/h



Molten aluminum feed "boils" on pool surface and is ejected by vapor pressure

Figure 2

Flash evaporation of Aluminum from Titanium

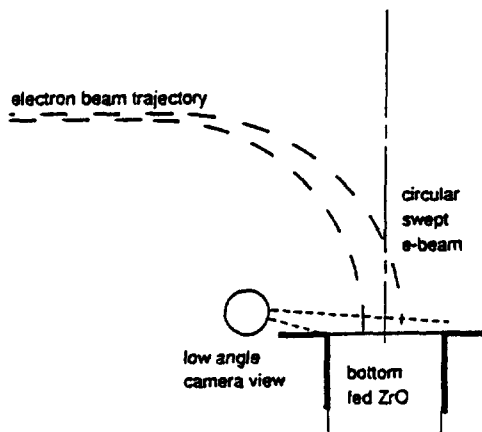


- E-gun power \cong 50 kW
- Ti vapor rate \cong 1.0 kg/h (based on diagnostic laser; verified by mass balance)
- Al wire feed rate \cong 0.56 kg/h

Molten aluminum feed droplet is swept along pool surface to pool edge

Figure 3

Vaporization of Zirconia

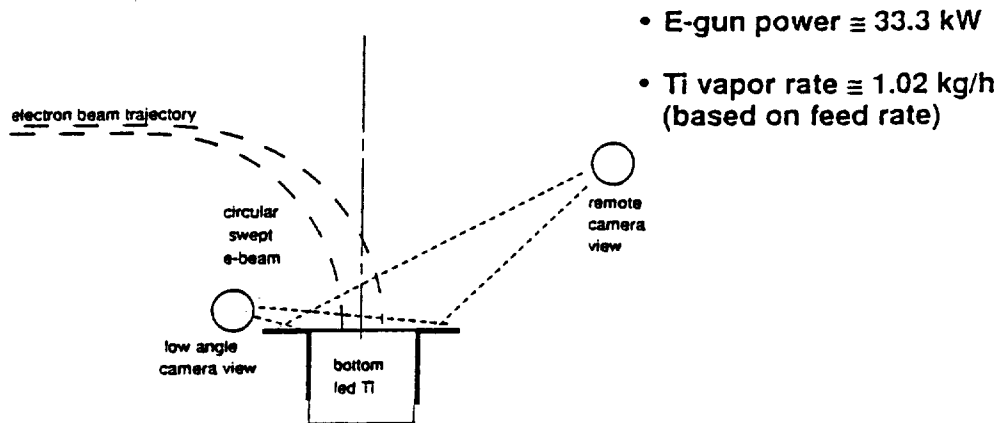


- E-gun power \cong 35 kW
- Average ZrO vapor rate \cong 0.86 kg/h (based on diagnostic laser)

Stable ZrO vaporization is achieved by careful monitoring of the ZrO source

Figure 4

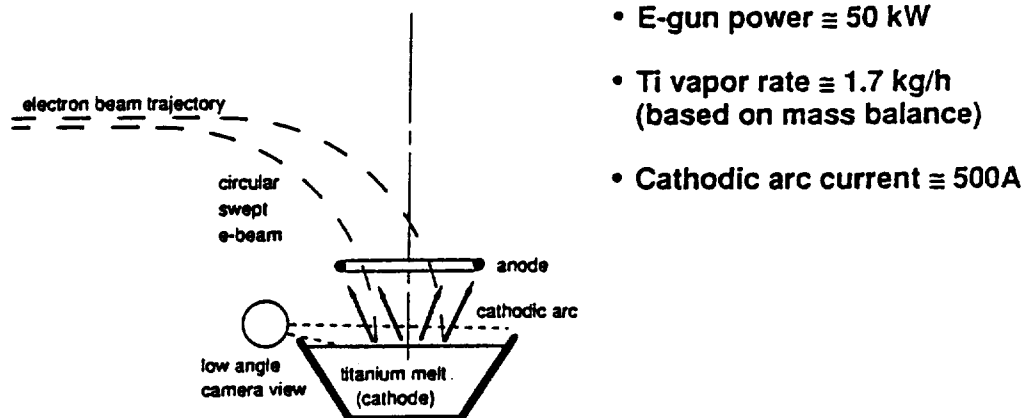
Titanium melt start-up



The low angle melt view confirms the calculated melt pool surface deformations at the liquid-vapor interface

Figure 5

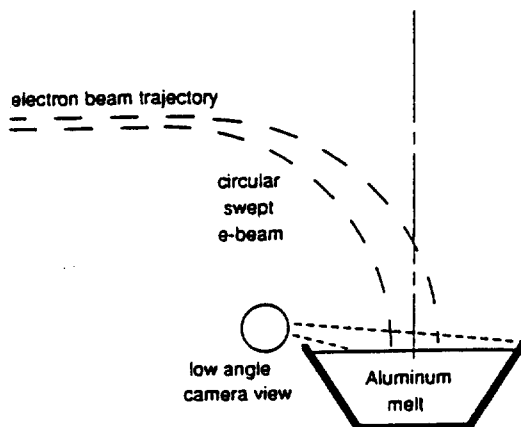
Titanium plasma arc



Cathodic arc conditions test "robustness" of video electronics; low angle melt video shows arc effects on vaporizer operation

Figure 6

Aluminum melt start-up



- E-gun power \cong 63 - 80 kW
- Aluminum vapor rate \cong 2.0 - 3.5 kg/h
(based on diagnostic laser;
verified by mass balance)

**Aluminum melt start-up conditons provide lower
limit for range of video imaging capability;
documents aluminum evaporation process conditions**

Technical Information Department • Lawrence Livermore National Laboratory
University of California • Livermore, California 94551

